Resonant and localized electromagnetic modes in finite superlattices

M. L. H. Lahlaouti,* A. Akjouj,† B. Djafari-Rouhani, and L. Dobrzynski
Laboratoire de Dynamique et Structures des Matériaux Moléculaires, UPRESA CNRS 8024, UFR de Physique, Université de Lille 1, F59655 Villeneuve d'Ascq Cedex, France

(Received 1 June 1998; revised manuscript received 17 February 1999)

The existence and behavior of surface and interface optical waves are studied in a substrate–finite-superlattice–air system. These modes appear as well-defined peaks in the density of states as well as in the magnitudes and phase times of the reflection and transmission coefficients. We investigate the effect of surface termination on the formation of surface modes and their interaction with the superlattice-substrate interface modes. The plot of the spatial distribution of the modes shows different possibilities of the guidance through the localized and confined modes.

Excitations in superlattices (SL's) with various stacking order, such as periodic, quasiperiodic, and random SL's, have been investigated extensively during the past decade. In these artificial media, composed of alternating layers of different materials with thicknesses of approximately 1–500 nm, the collective excitations that define their physical properties (phonons, plasmons, polaritons, magnons) are now very well studied phenomena.[1–4] Their fabrication has been performed by use of modern crystal-growth techniques (such as molecular-beam epitaxy), and because of their unusual properties, SL's are widely used in the design of optical and optoelectronic devices such as band-pass filters, mirrors, and quantum-well lasers.

The SL's actually grown are not ideal and they usually possess both natural and artificial defects. In particular, an inhomogeneity embedded in a SL with defect periodicity (e.g., a defect layer or a free surface) is shown to cause localized modes within the frequency gaps induced by the periodicity of the SL.[5–7] The existence of the electromagnetic modes localized at the surface of a SL was also predicted almost two decades ago.[8] Subsequently, experiments in a periodic layer structure which consisted of 12 pairs of alternating layers of GaAs and $Al_{0.2}Ga_{0.8}As$ on a GaAs substrate[9,10] and in ZnS/cryolite SL's (Ref. 11) proved their existence. On the theoretical side, it is also known that the presence of a SL/air interface[12–15] and SL/substrate interface[14] gives rise to localized states inside the gaps. The localized electromagnetic modes due to defect layers have also been studied for both infinite- and finite-size SL systems.[5–7] These properties started also to be investigated in two-dimensional (2D) and 3D photonic crystals.[16–18] These localized modes in the forbidden band can be used to manufacture semiconductor microlasers with almost perfect quantum efficiency and extremely low threshold.[19]

In this paper, we study the existence and behavior of the localized and resonant waves in the realistic geometry of a finite superlattice bounded by a substrate and the vacuum. The surface of the superlattice may be covered by a cap layer as in usual experimental situations (see Fig. 1). From the methodological point of view, this paper contains an extension of a previous work,[14] dealing with semiinfinite superlattices, to the case of a finite superlattice. However, in this more general and realistic situation, one can simultaneously encounter both surface and interface modes as well as confined modes in the finite superlattice. Moreover, these modes can interact together and give rise, for instance, to an anticrossing between a pair of surface and interface dispersion curves with a transfer of character from one branch to the other. On the other hand, we shall show that the thickness of the cap layer deposited on the superlattice will strongly influence the existence and behavior of surface modes and their interaction with interface and confined modes.

The localized and resonant modes manifest themselves through the density of states as well as through the rates and phase times of the transmission and reflection coefficients. Among different mathematical approaches, the Green-function method is quite suitable for studying the spectral properties of these composite materials; in particular, it enables us to calculate the local and total density of states (DOS) in which the resonant modes appear as well-defined peaks. Simultaneously, the Green-function approach allows us also to determine the transmission and reflection rates as well as the corresponding phase times. The phase times are considered[20] to be relevant physical times to describe the motion of wave packets which are narrow in wave-number space. We show that the positions of the resonances obtained from the DOS coincide with those given by phase times and transmission rates. The half-width of the peaks in the DOS

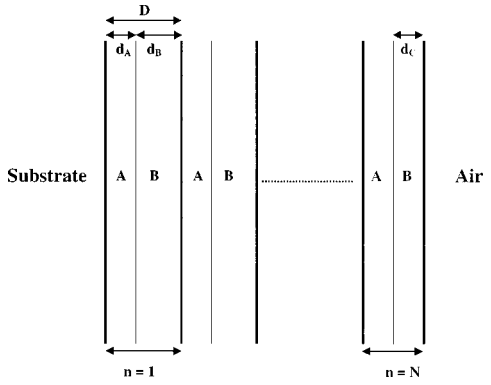

FIG. 1. Schematic representation of the system consisting of a substrate and a finite periodic superlattice with alternate stacking of *A* and *B* layers and capped with a *B* layer. *N* denotes the number of cells.

and phase times are related to the lifetime of the resonant modes. While the amplitudes and phase factors of the reflection and transmission coefficients can be measured experimentally, the DOS contains information about the spatial distribution of the modes and their localization behavior, for example they allow us to specify the surface, interface, confined, or mixed character of the modes.

The Green's function [from which the total DOS, local DOS (LDOS), phase times, and reflection and transmission rates are deduced] is calculated by using the interface response theory[21] in composite materials in which the solution is first searched in the restricted space of the interfaces before being extended to the whole material. We avoid the detail of the analysis, which is similar to, although more cumbersome than, that for a semi-infinite SL.[14] The complete Green's functions can also be used to derive any other physical property of the system at hand. They play a central role in the theories of light scattering (both Brillouin and Raman), as well as in various other physical phenomena.[22]

The Green's function is calculated by using the interface response theory in composite materials and is given as[21]

$$g(DD)=G(DD)-G(DM)G^{-1}(MM)G(MD) + G(DM)G^{-1}(MM)g(MM)G^{-1}(MM)G(MD), \tag{1}$$

where D and M are, respectively, the whole space and the space of the interfaces in the composite materials; $G(DD)$ is the block-diagonal matrix in which each block G_i corresponds to the bulk Green function of the subsystem i. In our case, the SL is composed of slabs of materials $i=A,B$. $g(MM)$ are the interface elements of the Green's function of the composite system. The inverse $g^{-1}(MM)$ of $g(MM)$ is obtained for any points in the space of interfaces as a superposition of the different $g_i^{-1}(M_iM_i)$, inverse of the $g_i(M_iM_i)$ for each constituent i of the composite system. In the geometry of the SL, the elements of the Green's function take the form $g(\omega,k_\parallel/x_3,x_3')$, where ω is the frequency of the electromagnetic wave, $k_\parallel$ the modulus of the wave vector parallel to the interface, and x_3 indicates the position along the SL axis.

Knowing the Green's function, one can obtain for a given value of $k_\parallel$ the local and total density of states. The local density of states on the plane (n,i,x_3) is given by

$$n(\omega^2,k_\parallel;n,i,x_3)=-\frac{\varepsilon_i}{\pi c^2}\,\mathrm{Im}\,g^+(\omega^2,k_\parallel;n,i,x_3;n,i,x_3), \tag{2}$$

where

$$g^+(\omega^2)=\lim_{\Gamma\to 0}[g(\omega^2+i\Gamma)], \tag{3}$$

c is the speed of light, n the index of the cell of the SL, and ε_i the dielectric function of the medium i. The total density of states for a given value of $k_\parallel$ is obtained by integrating over x_3 and summing over n and i the local density of states.

Moreover, if $U(D)$ represents an eigenvector of the reference system, Eq. (4) enables one to calculate the eigenvectors $u(D)$ of the composite materials,[21]

$$u(D)=U(D)-U(M)G^{-1}(MM)G(MD) + U(M)G^{-1}(MM)g(MM)G^{-1}(MM)G(MD). \tag{4}$$

This equation enables one also to calculate all the waves reflected and transmitted by the interfaces as well as the reflection and transmission coefficients of the composite system. One can deduce the photon phase times, which are defined in the stationary phase approximation, by[20]

$$\tau_R=\frac{d\theta_R}{d\omega} \quad \text{or} \quad \tau_T=\frac{d\theta_T}{d\omega}, \tag{5}$$

where θ_R and θ_T are, respectively, the phases of the reflected and transmitted amplitude of photons scattered off the substrate/SL/air.

The idea of the phase times (together with other characteristic times) has been introduced in connection with the question of how much time it takes a particle to tunnel across—or to be reflected from—a barrier.[23] It has been shown that the phase times defined in Eq. (5) are well suited to describe the delay time for the arrival of the maximum of the transmitted or reflected wave packet.[24–26] Furthermore, the time-independent Schrödinger equation and the Helmholtz wave equation describing the propagation of monochromatic electromagnetic waves are formally equivalent.[27] Therefore, the electronic tunnel effect and the frustrated optical transmission phenomena were shown to be related.[27,28]

These quantities, τ_R and τ_T, are of great interest because they are measurable quantities and furthermore they can be related to the density of states, which is a central quantity in the understanding of many phenomena in different physical systems. More precisely, following the demonstration by Avishai *et al.*,[29] one can easily show in our system[30] that the transmission phase time and the density of states are directly related through

$$\tau_T=\pi\Delta n. \tag{6}$$

Here Δn is the density of states of our system, from which the contributions of the substrate alone and the vacuum have been subtracted. Then, it is not surprising that the same features appear both in the density of states and in the transmission phase time, except that the transmission coefficient can only be defined when the frequency of the incident wave falls above the vacuum light line. On the other hand, there is not, in general, a simple relationship between the reflection phase time and the density of states, although in practice, in most of the situations, the peaks in the density of states also appear as well-defined features in τ_R.

However, let us notice that τ_R and Δn are directly related in two particular cases,[30] as follows: (i) for a symmetric system (i.e., a symmetric superlattice bounded by the same substrate on both sides),

$$\tau_R=\tau_T=\pi\Delta n; \tag{7}$$

(ii) in the case of total reflection (which means that the frequency of the incident wave falls below the vacuum light line),

$$\tau_R=2\pi\Delta n. \tag{8}$$

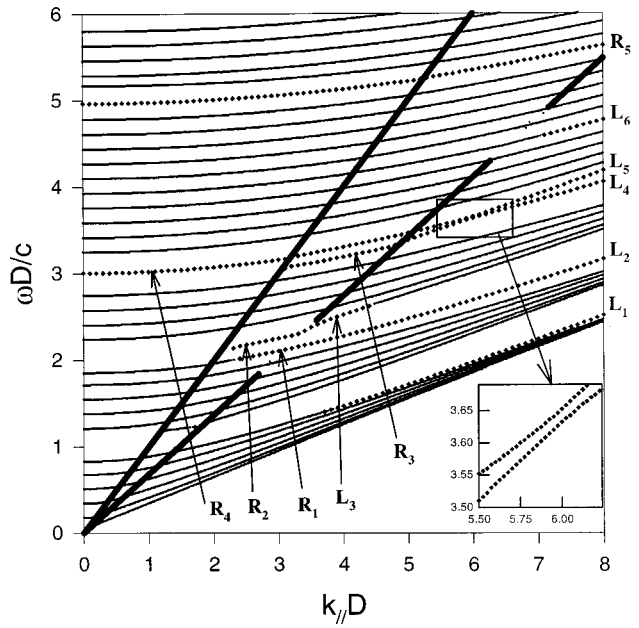

FIG. 2. Dispersion of electromagnetic modes associated with a finite SL sandwiched between a substrate and air. The SL contains $N=6$ cells. The dashed-dotted (full) heavy line corresponds to the substrate (air) velocity line, separating the confined modes in the SL from their extension as resonant modes into the substrate bulk band. The full lines give the dispersion of the SL minibands. The dotted lines give the localized (L_i) and resonant (R_i) modes inside the SL gaps.

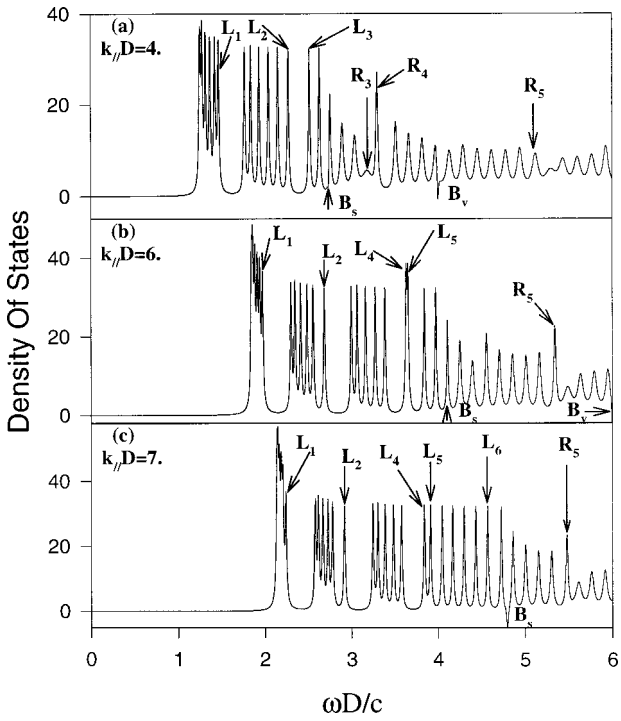

FIG. 3. Variation of the density of states (in units of D/c) corresponding to the case depicted in Fig. 2, for $k_{\|}D=4$ (a), 6 (b), and 7 (c). $B_s(B_v)$ refers to the δ function of weight $-\frac{1}{4}$ appearing at the bottom of the substrate (air) bulk band. R_i and L_i refer to the resonant and localized modes.

In what follows, we shall focus on a few applications of these results. Specific results will be given for a finite SL constituted of alternating TiO_2 and InGaAsP layers with a surface InGaAsP cap layer of different thickness and sandwiched between a substrate of SiO_2 and air. Let us mention that the TiO_2/SiO_2 materials were recently used in the construction of a Fibonacci quasiperiodic superlattice,[6,15] where the dispersion relation was investigated by an interferometric process; they were also used as a tunnel barrier to study the tunneling of optical pulses through the photonic band gaps.[26,31,32] On the other hand, calculations were performed for a $Au/SiO_2/InGaAsP/InP$ periodic optical waveguide to observe the eigenvalue modes of photons propagating through such a system.[33] In our calculation, we use the values of the dielectric constants given in the above works, namely $\varepsilon_A=5.5225$, $\varepsilon_B=12.39$, $\varepsilon_S=2.1316$, and $\varepsilon_0=1$ for TiO_2, InGaAsP, SiO_2 and air, respectively. Actually, these dielectric constants are complex quantities which also display some variation with the frequency of the light. These dispersion and absorption effects can formally be included in our calculation for a quantitative purpose; however, in this paper we limit ourselves to a more qualitative description of the behavior of the surface and interface electromagnetic waves, and therefore we assume the dielectric constants to be real and independent of the frequency. The materials used in our calculation correspond to a relatively high dielectric contrast ($\varepsilon_B/\varepsilon_A=5.8$), which insures the existence of relatively large minigaps. The geometrical parameters of the superlattice are defined in the following way. The thicknesses of the layers are denoted d_A and d_B, and D is the period of the superlattice $D=d_A+d_B$. For the sake of clarity, the SL contains $N=6$ layers of a dielectric A and $N-1=5$ layers of dielectric B and is capped with a B dielectric layer of thickness d_C. The numerical calculations are performed for $d_B=2d_A=2D/3$ and $d_C=0.57D$. In this work, we concern ourselves with the TE waves. The treatment of the TM waves is similar. The results that we shall discuss provide the general qualitative behavior of the localized and resonant modes that we also found in calculations with other constitutive materials for the SL.

Figure 2 gives the dispersion curves (dimensionless frequency $\omega D/c$ versus the reduced wave vector $k_{\|}D$) for TE waves in the structure depicted above. The localized and resonant discrete modes are induced by the substrate–finite-SL–cap-layer–air interactions and they are very sensitive to the thicknesses and to the nature of the SL layers. They are obtained from the maxima of the peaks in the total DOS (see Fig. 3). In Fig. 2, we plot two light lines: the air light line (heavy line) given by the equation $k_{\|}D=\omega D\sqrt{\varepsilon_0}/c$, and the substrate light line (heavy dashed line) given by the equation $k_{\|}D=\omega D\sqrt{\varepsilon_s}/c$. These lines delimit the oscillatory and the decaying behavior of the field in air or in the substrate. The branches situated below the substrate light line correspond either to the confined modes in the finite SL region or to the localized modes at the boundaries of the SL; they decay exponentially both into the substrate and into air. The extension of these curves into the substrate band (continuum) represents resonant modes associated with the deposition of the finite SL on the top of the substrate.

The branches represented by the full lines correspond to the confined modes of the finite SL; their number increases with the number N of periods in the SL, leading to the bulk

bands of the infinite SL in the limit $N \to \infty$. The branches represented by the dotted lines, and falling in the minigaps of the SL, are localized and resonant modes; they are mainly localized at the SL-substrate or SL-air interfaces. In the following, we shall concentrate on the discussion of the latter modes, which are very sensitive to the physical parameters of the SL layers but also to the SL termination and more especially to the position of the SL surface (i.e., SL/air interface).

In Fig. 2, there are six branches (dotted lines) of localized modes situated below the substrate bulk band and falling inside the gaps of the SL. The localization properties of these modes will be discussed below. The lowest localized branch (L_1) is a surface mode which emerges from the first miniband of the SL at $k_{\parallel}D \approx 3.5$; in the same manner, the surface localized branch (L_2) appears on the top of the second miniband when $k_{\parallel}D \geqslant 2.5$. Similarly, the lowest branch of the third SL miniband becomes the localized mode (L_3) when $k_{\parallel}D \leqslant 4.5$. The two localized modes L_4 and L_5 existing inside the third minigap of the SL are associated with one surface mode and one interface mode, which strongly interact around $k_{\parallel}D \approx 6$ giving rise to an anticrossing in the dispersion curves. Finally, the branches falling above the substrate light line correspond to resonant modes as they can propagate in the substrate.

A few examples of the behavior in the variation of the DOS of the resonant modes are illustrated in Fig. 3, for $k_{\parallel}D = 4$ (a), 6 (b), and 7 (c). Let us notice that the δ peaks lying below B_s are enlarged by adding a small imaginary part to the frequency ω. The peaks that lie below B_s represent confined modes inside the SL or localized modes (L_i) at the interfaces of the SL, and decay on both sides of the SL; those lying between B_s and B_v may propagate in both the SL and the substrate and those falling above B_v are propagating in the whole composite system. R_i and L_i refer to the resonant and localized modes in the system. Let us recall[14] that the δ peaks of weight $-\frac{1}{4}$ appearing at the bottom of the substrate and air bands correspond to the variations in the total DOS when these media are going from infinite (bulk) to semi-infinite.

Depending on their frequencies, the optical modes induced by the finite SL may propagate along the x_3 direction perpendicular to the interfaces in the SL, the cap layer, and the substrate, they may propagate in one and decay in the other, or finally they may decay on both sides of the SL/substrate and SL/air interfaces. To illustrate these different types of behavior, we have plotted in Figs. 4(a)–4(e) the local densities of states (LDOS) as a function of the x_3 space position for $k_{\parallel}D = 6$ and for different reduced frequencies $\omega D/c = 1.975$ (a), $\omega D/c = 2.69$ (b), $\omega D/c = 3.39$ (c), $\omega D/c = 3.635$ (d), and $\omega D/c = 3.655$ (e). The LDOS reflects the spatial behavior of the square modulus of the electric field.

In the first two cases [Figs. 4(a) and 4(b)], the frequencies correspond, respectively, to L_1 and L_2 in Fig. 2. They reflect guided modes of the cap layer, which decay outside this layer, with a small penetration into the SL. In the case (c), the frequency falls inside a miniband of the SL while being below the substrate bulk band; therefore, this corresponds to a confined mode inside the finite SL. The last two cases (d) and (e) correspond, respectively, to the modes L_4 and L_5 in Figs. 2 and 3(b). The corresponding LDOS show a decaying behavior inside the SL from both substrate/SL and SL/cap-layer interfaces. Due to the interaction between these two modes, their wave functions are distributed on both sides of the SL with a slightly bigger weight at the substrate/SL interface. Furthermore, using the LDOS, we note that as far as $k_{\parallel}D \geqslant 6$, the branches L_4 and L_5 correspond, respectively, to a mode localized in the SL/cap layer and a mode localized at the substrate/SL interface; after their interaction at the anticrossing point around $k_{\parallel}D = 6$, they change their localization character and become, respectively, localized at the substrate/SL and the SL/cap-layer interfaces. At the anticrossing point, there is a transfer between the character of the modes. In the same manner, with the help of the LDOS, we can notice that the branches L_3 and L_6 in Fig. 2 correspond to modes localized at the substrate/SL interface as their LDOS decay exponentially from this interface.

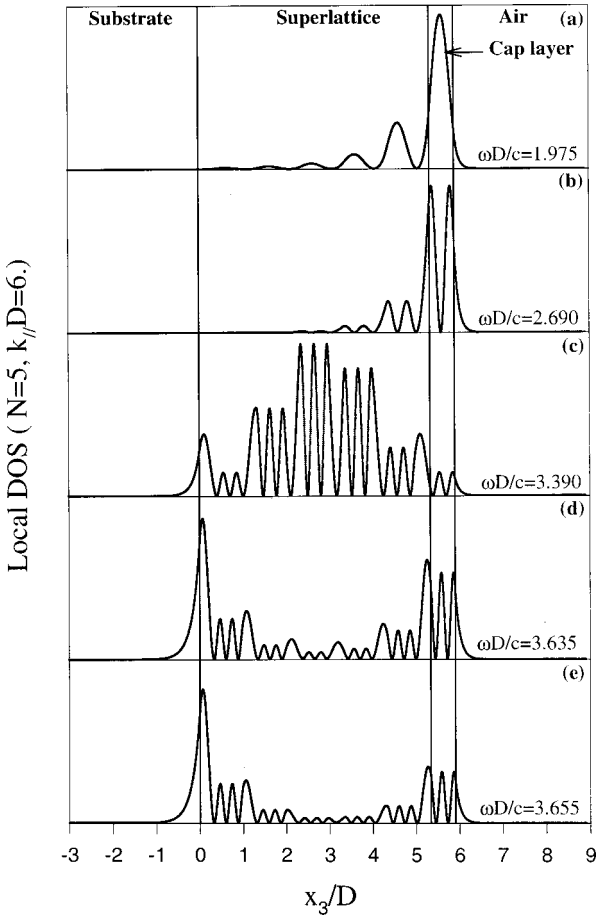

FIG. 4. Spatial representation of the local density of states corresponding to the case depicted in Fig. 2, for $k_{\parallel}D = 6$ and for different reduced frequencies $\omega D/c = 1.975$ (a), $\omega D/c = 2.69$ (b), $\omega D/c = 3.39$ (c), $\omega D/c = 3.635$ (d), and $\omega D/c = 3.655$ (e).

Next, we discuss the comparison between the DOS and the transmission and reflection phase times. Figure 5 presents the frequency dependence of the variation of the DOS (a), the transmission rate (b), the transmission phase time (c), and the reflection phase time (d), for $k_{\parallel}D = 3.2$. The incident wave from the substrate is represented by a plane wave. The incident photons are scattered from the interfaces between the dissimilar layers constituting the system. The transmission rate [Fig. 5(b)] shows sharp peaks with frequency positions corresponding to the peaks in the DOS [Fig. 5(a)]. The transmission drops exponentially in the gap of the SL and

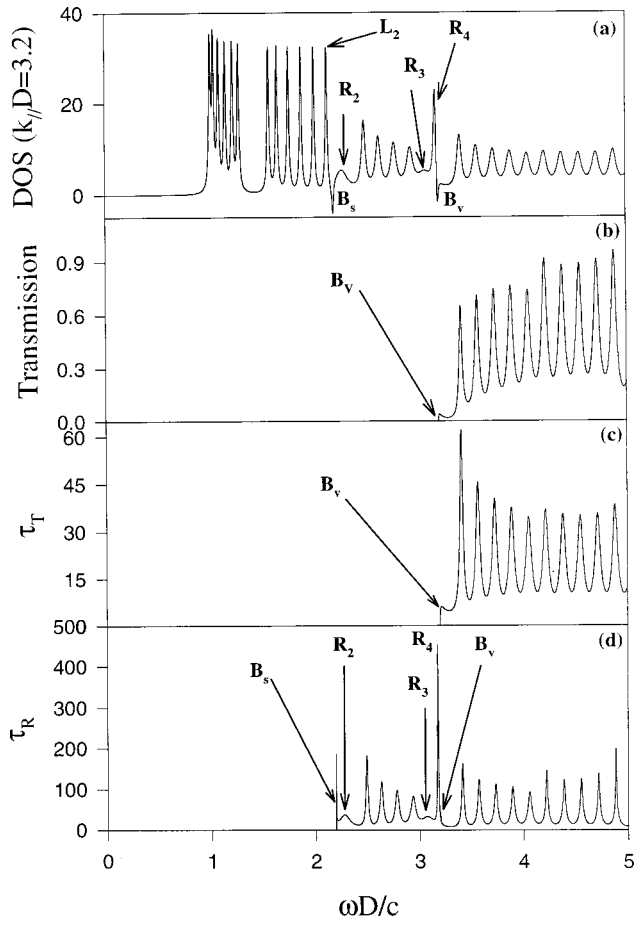

FIG. 5. Frequency dependence of the DOS (a), the transmission coefficient (b), the transmission phase time (c), and reflection phase time (d) for $k_{\|}D=3.2$ The geometrical parameters are the same as in Fig. 2.

this decay becomes more important by increasing the number N of cells in the SL. It is worth noting that below B_v, there is no transmission and therefore the transmission coefficient is zero. Let us notice that the sum of the reflection and transmission rates is equal to 1 for any value of the frequency, as it should be. An analysis of the phase times of the transmitted and reflected photon from the SL [Figs. 5(c) and 5(d)] shows that the transmitted and reflected phase times have the same behavior as the DOS for frequencies lying above B_v. It is interesting to notice that, contrary to the transmission rate and the transmitted phase time, the reflection phase time enables us to observe the resonance peaks lying between B_s and B_v, where the phenomenon of total reflection takes place. To illustrate the order of magnitude of the phase times, one can consider the case of a superlattice with period $D=300$ Å. The most significant resonance in Fig. 5 displays phase times of the order of 100 to 500 in units of D/c, which means $\tau=10-50$ fs, and falls in the range of the available experimental techniques.[26,31,32] However, the phase times associated with other resonances, in particular those corresponding to the confined modes of the superlattice, are in general too short to be accessed by experiment.

Finally, we investigate how the position of the SL surface (i.e., SL/air interface) affects the localized mode eigenfrequencies. We consider here the case of the finite SL with

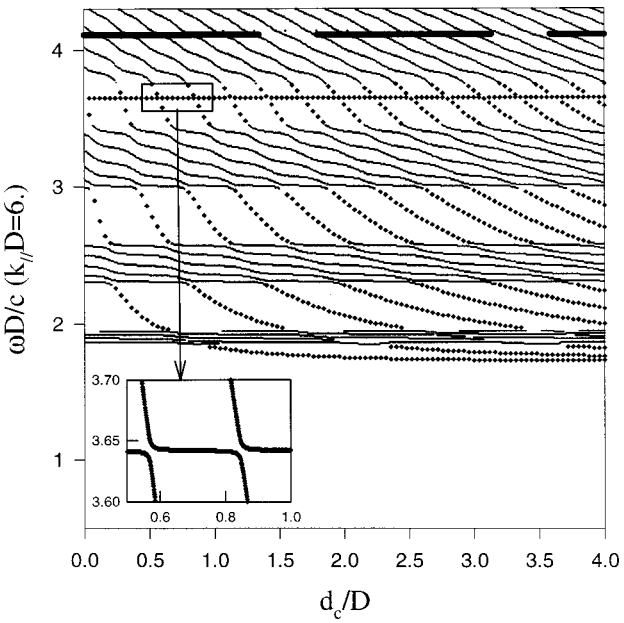

FIG. 6. Variation of the frequencies of the modes versus the thickness of the last layer of the SL (i.e., SL/air interface) for $k_{\|}D=6$. The SL contains $N=6$ layers of dielectric A and $N=5$ layers of dielectric B and is capped with a dielectric B layer of thickness d_c. The heavy dashed line indicates the velocity line of the substrate.

$N=6$ layers of dielectric A and $N-1=5$ layers of dielectric B and capped with a B dielectric layer of thickness d_c. Figure 6 shows the frequency of the optical modes as a function of d_c for $k_{\|}D=6$; the localized modes are represented by dotted square lines. The horizontal branch situated in the third gap of the SL corresponds to the localized modes at the substrate/SL interface. This mode remains insensitive to the variation of the surface layer and keeps a constant value for different values of d_c. The other branches situated inside the different SL gaps and below the substrate light line correspond to localized modes at the SL/air interface. They emerge from a SL bulk band for given values of d_c. A study of the local density of states shows that these modes are confined in the vicinity of the surface layer for $d_c>d_B$. In the limit of $d_c/D\rightarrow\infty$, their asymptotic value is $\omega D\sqrt{\varepsilon_B}/c$. Let us mention that, for any given frequency ω in Fig. 6, there is a periodic repetition of the resonant and of the surface modes as a function of d_c. We can also note that when d_c increases, the frequencies of the existing localized (respectively resonant) modes decrease until the corresponding branches merge into the lower miniband of the SL and become confined modes of the SL. Moreover, we observe in the third gap anticrossings at certain values of d_c between the branches corresponding to the substrate/SL and SL/air interface modes. At these anticrossing points, there is an interaction between the surface and interface modes with a transfer between the localization character of the two branches; at these anticrossing points, the weights of the two modes are distributed on both sides of the SL. Two examples of anticrossings at $d_c/D\approx0.57$ and 0.85 are presented in the inset of Fig. 6.

In summary, we have found well-defined peaks in the

DOS and phase times associated with resonant modes in a TiO_2-InGaAsP superlattice, even though these modes are in resonance with the bulk modes of the SiO_2 substrate. The intensity of the peaks in the DOS and phase times depends strongly on the number N of the SL cells and on the width and nature of the SL layers. The intensity of the peaks in the phase time describes the time needed for electromagnetic waves to complete the reflection or transmission process, while the DOS gives the weight of the resonances. We have also presented a study of the effect of the finite dielectric SL termination on the formation of the localized and resonant modes. It has been found that the occurrence, the position, and the localization properties of electromagnetic modes inside photonic band gaps are very sensitive to the surface termination of the SL layer, with the possibility of an anticrossing between a surface and interface mode. When the thickness of the surface layer varies, the interface modes move across the gaps from one SL band to the other.

Note added in proof. Recently, the surface and guided electromagnetic waves have been determined experimentally for different values of the wave vector in a TiO_2/SiO_2 superlattice (15 cells) deposited on a glass substrate.[34]

One of us (M.L.H.L.) gratefully acknowledges the hospitality of the Laboratoire de Dynamique et Structures des Matériaux Moléculaires, Université de Lille 1. His work was partially supported by Faculté des Sciences, Université A. Essaadi, Tétouan, Morocco.

*Permanent address: Département de Physique, Faculté des Sciences, B.P. 2121, Université Abdelmalek Essaadi, Tétouan, Morrocco.

†Corresponding author. Electronic address: akjouj@lip5rx.univ-lille1.fr

[1] R. E. Camley, B. Djafari-Rouhani, L. Dobrzynski, and A. A. Maradudin, Phys. Rev. B **27**, 7318 (1983).
[2] R. E. Camley and D. L. Mills, Phys. Rev. B **29**, 1695 (1984).
[3] E. L. Albuquerque and M. G. Cottam, Phys. Rep. **233**, 67 (1993).
[4] J. Barnas, J. Phys. C **21**, 4097 (1988).
[5] M. D. Tocci, M. Scalora, M. J. Bloemer, J. P. Dowling, and C. M. Bowden, Phys. Rev. A **53**, 2799 (1996).
[6] T. Hattori, N. Tsurumachi, and H. Nakatsuka, J. Opt. Soc. Am. B **14**, 348 (1997); T. Hattori, N. Tsurumachi, S. Kawato, and H. Nakatsuka, Phys. Rev. B **50**, 4220 (1994).
[7] Rongzhou Wang, Jinming Dong, and D. Y. Xing, Phys. Status Solidi B **200**, 529 (1997).
[8] P. Yeh, A. Yariv, and C. S. Hong, J. Opt. Soc. Am. **67**, 423 (1977).
[9] P. Yeh, A. Yariv, and A. Y. Cho, Appl. Phys. Lett. **32**, 104 (1978); P. Yeh, P. C. Chen, and A. Yariv, *ibid.* **32**, 370 (1978).
[10] P. Yeh, *Optical Waves in Layered Media* (Wiley, New York, 1988).
[11] A. A. Bulgakov and V. R. Kovtun, Opt. Spektrosk. **56**, 769 (1984) [Opt. Spectrosc. **56**, 471 (1984)].
[12] A. A. Bulgakov and V. R. Kovtun, Solid State Commun. **56**, 781 (1985).
[13] X. I. Saldana and G. Gonzalez de la Cruz, J. Opt. Soc. Am. A **8**, 36 (1991).
[14] M. L. Bah, A. Akjouj, E. H. El Boudouti, B Djafari-Rouhani, and L. Dobrzynski, J. Phys.: Condens. Matter **8**, 4171 (1996).
[15] F. Ramos-Mendieta and P. Halevi, J. Opt. Soc. Am. B **14**, 370 (1997).
[16] Y. F. Li and J. W. Y. Lit, J. Opt. Soc. Am. A **4**, 671 (1987).
[17] M. Sigalas, C. M. Soukoulis, E. N. Economou, C. T. Chan, and K. M. Ho, Phys. Rev. B **48**, 14 121 (1993).
[18] A. Mekis, J. C. Chen, I. Kurland, S. Fan, P. R. Villeneuve, and J. D. Jouannopoulos, Phys. Rev. Lett. **77**, 3787 (1996).
[19] E. Yablonovitch, Phys. Rev. Lett. **58**, 2059 (1987).
[20] E. H. Hauge, J. P. Falck, and T. A. Fjeldly, Phys. Rev. B **36**, 4203 (1987).
[21] L. Dobrzynski, Surf. Sci. Rep. **11**, 139 (1990).
[22] M. G. Cottam and A. A. Maradudin, in *Surface Excitations*, Modern Problems in Condensed Matter Science, Vol. 9 (North-Holland, Amsterdam, 1986), p. 5.
[23] E. H. Hauge and J. A. Støvneng, Rev. Mod. Phys. **61**, 917 (1989).
[24] A. Ranfagni, D. Mugnai, P. Fabeni, G. P. Pazzi, G. Naletto, and C. Sozzi, Physica B **175**, 283 (1991).
[25] S. Mizumo and S. Tamura, Phys. Rev. B **50**, 7708 (1994).
[26] V. Laude and P. Tournois, J. Opt. Soc. Am. B **16**, 194 (1999).
[27] R. Y. Chiao, P. G. Kwiat, and A. M. Steinberg, Physica B **175**, 257 (1991).
[28] B. Lee and W. Lee, J. Opt. Soc. Am. B **14**, 777 (1997).
[29] Y. Avishai and Y. B. Band, Phys. Rev. B **32**, 2674 (1985).
[30] M. L. H. Lahlaouti, A. Akjouj, B. Djafari-Rouhani, L. Dobrzynski, M. Hammouchi, E. H. El Boudouti, A. Nougaoui, and B. Kharbouch (unpublished).
[31] A. M. Steinberg, P. G. Kwiat, and R. Y. Chiao, Phys. Rev. Lett. **71**, 708 (1993).
[32] Ch. Spielman, R. Szipöcs, A. Stingl, and F. Krauss, Phys. Rev. Lett. **73**, 2308 (1994).
[33] Chunsheng Ma, J. Opt. Soc. Am. A **13**, 276 (1996).
[34] W. M. Robertson and S. May, Appl. Phys. Lett. **74**, 1800 (1999).